ATF2-3 Wakefield Mitigation Techniques, Past Studies and Future Plans

P. Korysko*, A. Latina

CLIC Mini Week
December 13, 2023

*pierre.korysko@cern.ch

Outline

- Intensity-dependent effects in ATF2
  - Simulations
    * Impact of static imperfections.
    * Impact of dynamic imperfections.
    * Impact of corrections (One-to-one, DFS, WFS)
  - Measurements
    * Impact of corrections (DFS, WFS, wakefield knobs).
    * Comparison between simulations and measurements.
- Experimental proposals

Simulations

Transverse and Longitudinal Wakefields

The integrated fields seen by a test particle traveling on the same, or on a parallel path at a constant distance s behind a point charge Q are called the integrated longitudinal and transverse wakepotentials. They are defined as:

$$\tilde{W}_{\perp}(\Delta r, s) = \frac{1}{Q}\int_0^L \left[E_{\perp}(\Delta r, z, s) + c\hat{z} \times B(\Delta r, z, s)\right] dz$$

$$\tilde{W}_{\parallel}(s) = -\frac{1}{Q}\int_0^L \left[E_z(z, s)\right] dz$$

The transverse and longitudinal kicks felt by a particle, at position z along the bunch, due to all leading particles ($\forall z' :\ z' > z$):

$$\Delta r' = \frac{\Delta P_{\perp}}{P} = \frac{qQL}{Pc}\int_{-\infty}^{z} W_{\perp}(\Delta r(z'), z - z')\,\rho(z')\,dz'$$

$$\Delta P_{\parallel} = \frac{qQL}{c}\int_{-\infty}^{z} W_{\parallel}(z - z')\,\rho(z')\,dz'$$

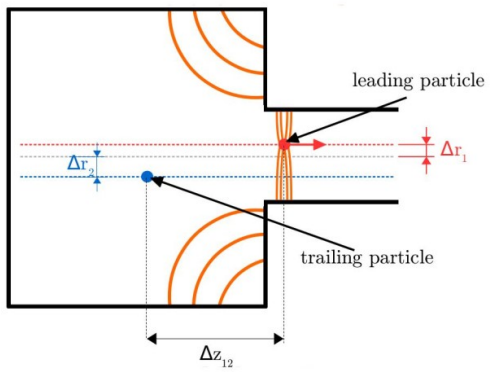

Figure: Scheme of the two-particle model.

with:

- $\rho(z')$ normalized line charge density of the bunch, such that $\int_{-\infty}^{\infty}\rho(z')\,dz' = 1$
- $\Delta r(z')$ transverse radial position of the leading particles as a function of their position z' along the bunch [mm]
- Q total charge of the bunch [C]
- q particle's charge [e]
- P particle's momentum [eV/c]
- $\Delta r'$ radial kick [rad]
- ΔP momentum loss [eV]

Corrections

One-to-One

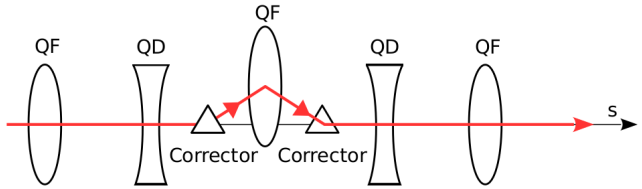

Figure : Schematic of the One-to-one correction. The beam orbit (in red) is deflected by correctors (triangles) in order to pass through the center of the BPM, which is inside a quadrupole in this case.

Dispersion Free Steering

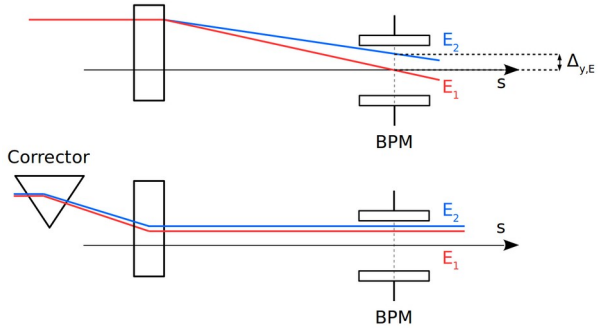

Figure: Schematic of the Dispersion Free Steering correction.

Wakefield Free Steering

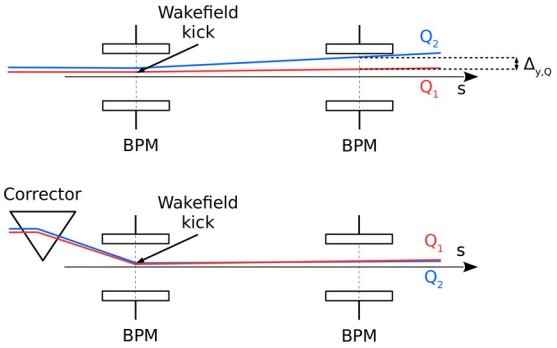

Knobs (Y, YP D XP XP.*XP XP.*YP XP.*D)

First order

Second order

Simulation conditions

- Wakefield sources: Cavity BPMs, bellows and flanges (wakepotentials calcultated with GdfidL).[7][8][9]

Position of wakefield sources

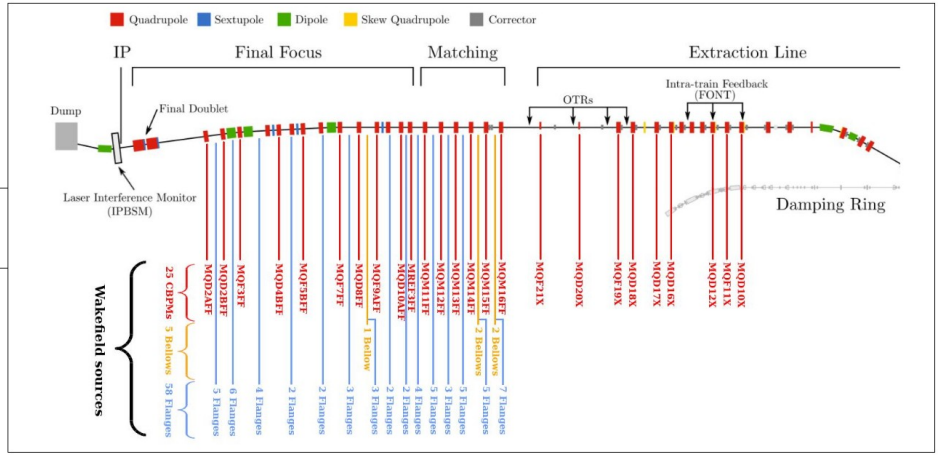

Wakefield sources wakepotentials (V/pC/mm)

Cavity BPM

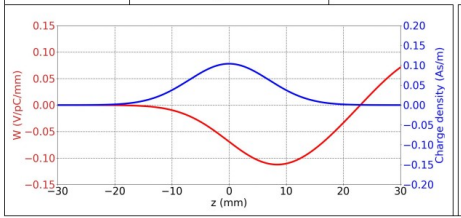

Bellows

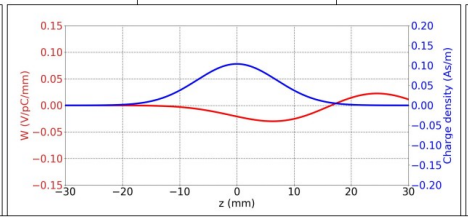

Flange

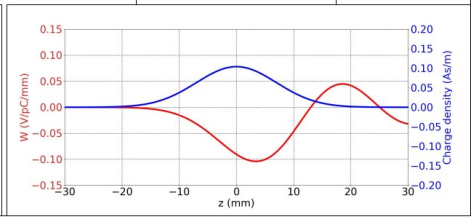

Simulation conditions

Simulated errors:

Static errors:
- Misalignement of quadrupoles, sextupoles and BPMs of 100 um RMS.

- Strength error of quadrupoles and sextupoles of 0.1% RMS.

- Roll error for quadrupoles and sextupoles of 200 urad RMS.

Dynamic errors:
- **Incoming pos./ang. jitter of [$0.1\sigma_{y/y'}$,-$1.0\sigma_{y/y'}$]**

Corrections applied:

- One-to-one
- DFS
- WFS
- Knobs (Y, YP D XP XP.*XP XP.*YP XP.*D)

First order

Second order

Simulation procedure:

Tracking 200 bunches per machine from the ATF extraction line to the IP.

100 machines with the previously cited static imperfections.

Apply the cited corrections and the knobs on the distribution at the IP.

Tracking code used: PLACET

Impact of orbit corrections

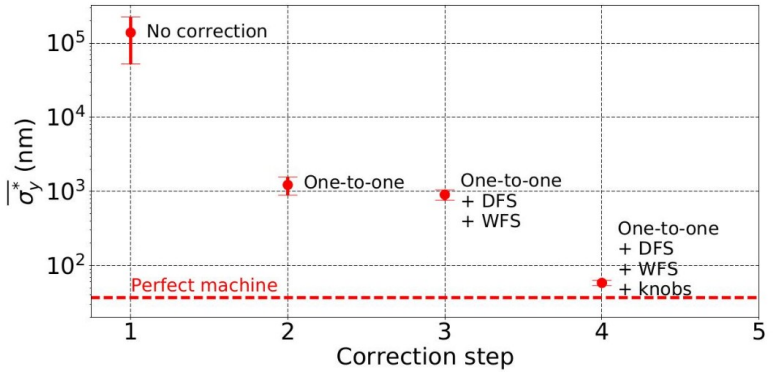

Figure : Average vertical beam size at the IP (σ_y^*) vs. correction step: One-to-one, DFS, WFS corrections and IP tuning knobs. The red dashed line show the vertical beam size at the IP for a perfect machine, 37 nm.

Correction	$\overline{\sigma_y^*}$
No correction	13.8 ± 86.2 µm
One-to-one	1220 ± 337 nm
One-to-one + DFS + WFS	904 ± 145 nm
One-to-one + DFS + WFS + knobs	58.4 ± 4.7 nm

Impact of static errors

Misalignement of quadrupoles, sextupoles, BPMs of 100 um RMS
Strength error of quadrupoles, sextupoles of 0.01% (+ misalignment 100 um)
Roll error for quadrupoles and sextupoles of 200 urad:

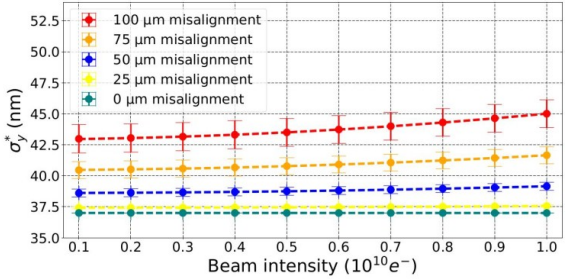

Figure: Effect of the misalignments on the vertical beam size at the IP (σ_y^*) vs. the beam intensity with wakefields calculated with PLACET.

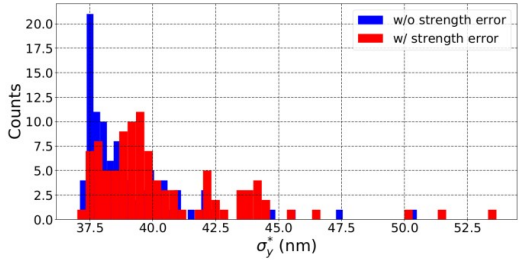

Figure : Effect of quadrupoles and sextupoles strength error of 10^{-4} RMS at $1.0 \times 10^{10} e^-$ on the vertical IP beam size (σ_y^*), in presence of wakefields calculated with PLACET.

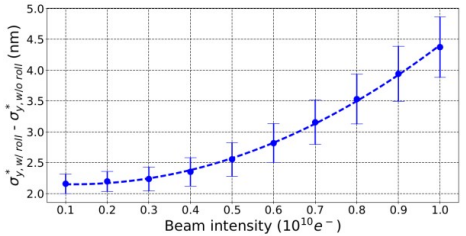

Figure: Effect of 200 μrad RMS rolls of BPMs, quadrupoles and sextupoles on the vertical IP beam size (σ_y^*) vs. the beam intensity, in presence of wakefields calculated with PLACET.

Static error	Misalignment	Strength error	Roll error
Error amplitude	100 [μm]	1×10^{-4}	200 [μrad]
Average σ_y^* at 10^9 e^- [nm]	43 ± 1.1	39 ± 0.09	39 ± 0.16
Average σ_y^* at 10^{10} e^- [nm]	45 ± 1.1	42 ± 0.29	41 ± 0.49

19

Impact of dynamic errors

Incoming position jitter of $[0.1\sigma_y - 0.5\sigma_y]$
Incoming angle jitter of $[0.1\sigma_{y'} - 0.5\sigma_{y'}]$
Incoming position/angle jitters of $[0.1\sigma_{y/y'} - 1.0\sigma_{y/y'}]$

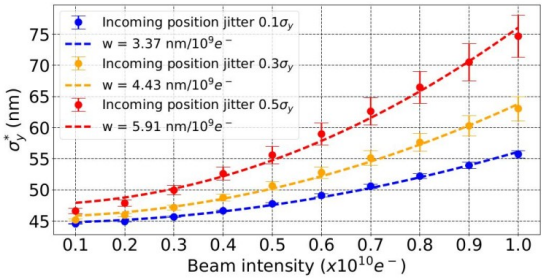

Figure: Effect of incoming 0.1, 0.3 and 0.5 σ_y beam position jitter on the vertical beam size at the IP (σ_y^*) vs. the beam intensity, calculated with PLACET in presence of wakefields.

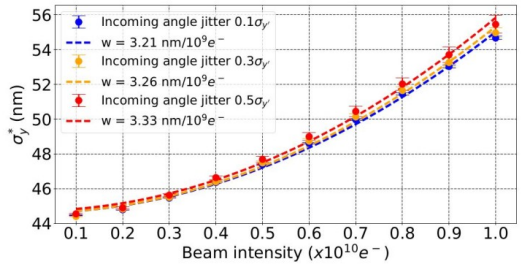

Figure: Effect of incoming 0.1, 0.3 and 0.5 $\sigma_{y'}$ beam angle jitter on the vertical beam size at the IP (σ_y^*) vs. the beam intensity, calculated with PLACET in presence of wakefields.

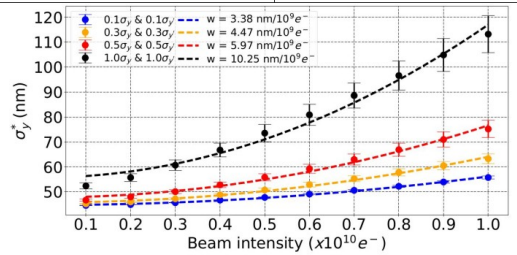

Figure: Effect of both incoming 0.1, 0.3, 0.5 and 1.0 σ_y beam position and 0.1, 0.3, 0.5 and 1.0 $\sigma_{y'}$ beam angle jitters on the vertical beam size at the IP (σ_y^*) vs. the beam intensity, calculated with PLACET in presence of wakefields.

$$w\,[nm/10^9] = (\sqrt{\sigma_{y,q}^2 - \sigma_{y,0}^2})/q$$

Impact of dynamic errors

Jitter	w [nm/10^9 e^-]	Intensity [e^-]	Average σ_y^* [nm]
Inc. pos. jitter $0.1\sigma_y$ and ang. jitter $0.1\sigma_{y'}$	3.4 ± 0.3	1.0×10^9 10.0×10^9	45.0 ± 0.1 56.0 ± 0.6
Inc. pos. jitter $0.3\sigma_y$ and ang. jitter $0.3\sigma_{y'}$	4.5 ± 0.5	1.0×10^9 10.0×10^9	45.0 ± 0.2 63.0 ± 2.0
Inc. pos. jit. $0.3\sigma_x$ & $0.3\sigma_y$ and ang. jit. $0.3\sigma_{x'}$ & $0.3\sigma_{y'}$	4.6 ± 0.6	1.0×10^9 10.0×10^9	45.0 ± 0.2 64.0 ± 2.1
Inc. pos. jitter $0.5\sigma_y$ and ang. jitter $0.5\sigma_{y'}$	6.0 ± 1.0	1.0×10^9 10.0×10^9	47.0 ± 0.4 75.0 ± 3.5
Inc. pos. jitter $1.0\sigma_y$ and ang. jitter $1.0\sigma_{y'}$	10.2 ± 2.8	1.0×10^9 10.0×10^9	52.0 ± 1.2 113.0 ± 7.4

Static error	Misalignment	Strength error	Roll error
Error amplitude	100 [μm]	1×10^{-4}	200 [μrad]
σ_y^* growth at 10^9 e^-	16%	4%	6%
σ_y^* growth at 10^{10} e^-	22%	15%	12%
Dynamic error	**Angle jitter**	**Position jitter**	Both jitters
Error amplitude	$0.5\sigma_{y'}$	$0.5\sigma_y$	$0.5\sigma_y$ and $0.5\sigma_{y'}$
σ_y^* growth at 10^9 e^-	22%	27%	27%
σ_y^* growth at 10^{10} e^-	49%	103%	103%

Wakefield Knobs – Experimental Setup

Position: The setup was installed in the the ATF2 extraction line between QD10BFF and QD10AFF. The phase between the setup and the IP is around 2.5π. Thus, the kicks generated by the setup translate into a position offset at IP.

Goal: Use two well known wakefield sources on movers in the ATF2 extraction line to compensate the intensity-dependent effects.
Setup: Made of two movers, the first one carries two C-BPMs and the second one carries a bellows.

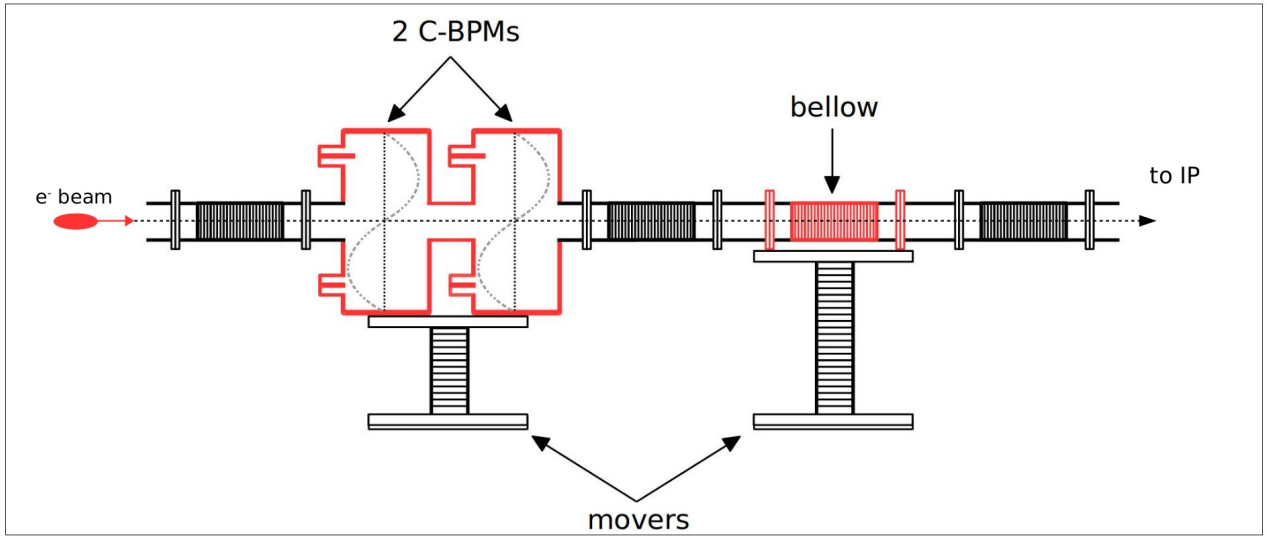

Wakefield Knobs – Results

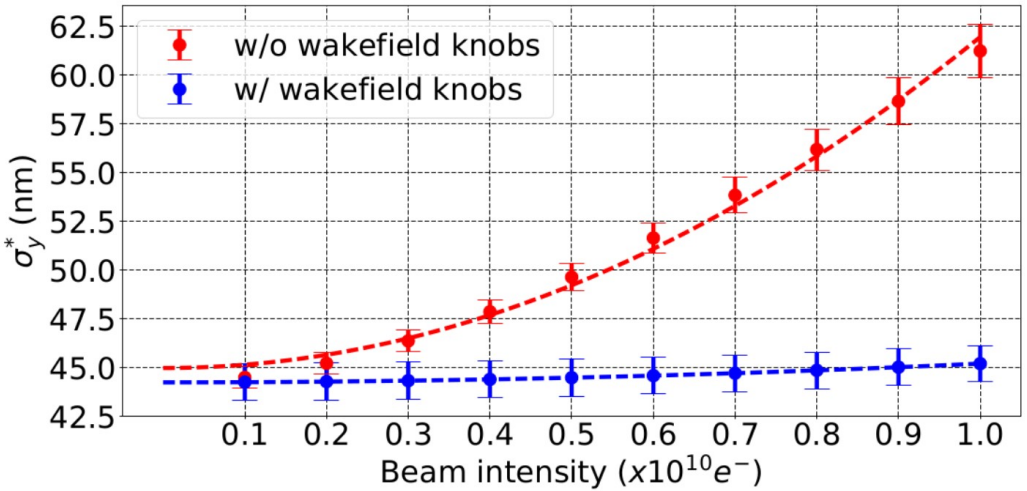

Figure: Simulations of the impact of the ATF2 wakefield knobs on the vertical IP beam size (σ_y^*).

Case	$\overline{\sigma_y^*}$ [nm]
No source on movers	61.2 ± 1.4
Using the bellow on mover	48.4 ± 1.0
Using the 2 C-BPMS on mover	45.5 ± 0.9
Using both the bellow and the 2 C-BPMs on movers	45.2 ± 0.9

Measurements

Impact of corrections (DFS and WFS)

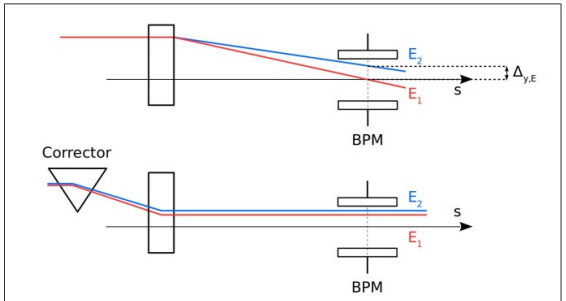

Figure: Schematic of the Dispersion Free Steering correction.

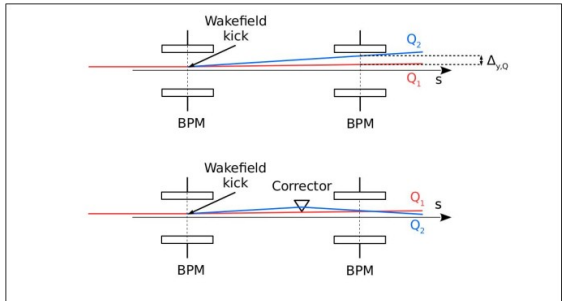

Figure: Schematic of the Wakefields Free Steering corrections.

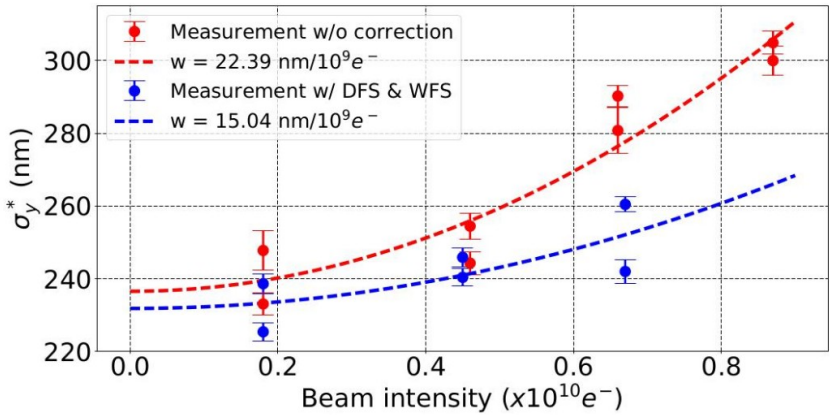

Figure: Measurement: impact of DFS and WFS on the vertical beam size at the IP.

Impact of corrections (Wakefield Knobs)

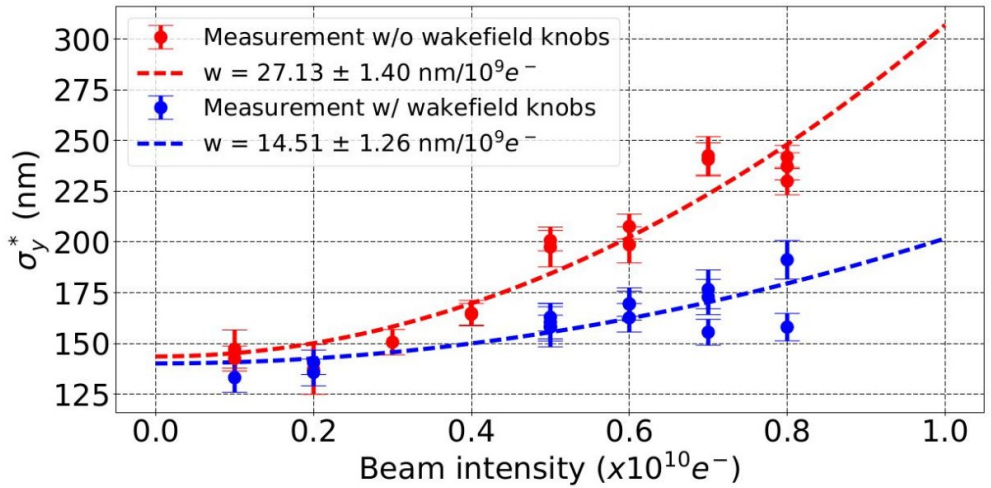

Figure : Measured vertical IP beam size (σ_y^*) vs. the beam intensity before and after applying wakefield knobs.

$$w[nm/10^9] = (\sqrt{\sigma_{y,q}^2 - \sigma_{y,0}^2})/q$$

*Using the IPBSM 30° mode

The wakefield knobs reduced the intensity dependence parameter from **27.13 nm/10^9** to **14.51 nm/10^9**. (The **IP angle jitter** was **70 urad**).

Comparisson Simulations/Measurements

Simulations:

Static errors:
- Misalignement of quadrupoles, sextupoles and BPMs of 100 um RMS.
- Strength error of quadrupoles and sextupoles of 0.1% RMS.
- Roll error for quadrupoles and sextupoles of 200 urad RMS.

Dynamic errors:
- Incoming pos. & ang. jitter of $1.0\sigma_y$ and $1.0\sigma_{y'}$ respectively.

Measurements:

Done on 03/02/2016 (Intensity_fringe_160203_193347)

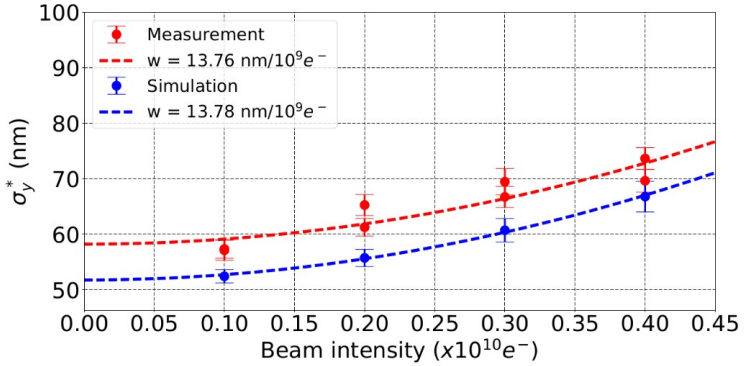

Figure: Comparison between measurements and simulations of the vertical beam size at the IP (σ_y^*) vs. the beam intensity and the intensity-dependent parameter w.

Case	w [nm/10^9 e^-]	Beam intensity [e^-]	$\overline{\sigma_y^*}$ [nm]
Meas	13.8 ± 1.6	0.1×10^{10}	57.0 ± 1.7
		0.2×10^{10}	63.0 ± 1.7
		0.3×10^{10}	68.0 ± 2.1
		0.4×10^{10}	72.0 ± 2.0
Sim	13.8 ± 0.3	0.1×10^{10}	52.0 ± 1.2
		0.2×10^{10}	56.0 ± 1.6
		0.3×10^{10}	61.0 ± 2.1
		0.4×10^{10}	67.0 ± 2.8

Good agreement between measurements and simulations for the intensity-dependent effects.

SVD analysis - Measurements

$$D = \begin{pmatrix} d_{11} & d_{12} & \cdots & d_{1N} & q_1 \\ d_{21} & d_{22} & \cdots & d_{2N} & q_2 \\ \vdots & \vdots & & \vdots & \vdots \\ d_{M1} & d_{M2} & \cdots & d_{MN} & q_M \end{pmatrix}$$

Adding charge information

d_{ik} = measured displacement in BPM k for machine pulse i
M = number of machine pulses
N = number of BPMs
q = charge of pulse i

Reconstructed matrix D_q keeping only 5th singular value

$$S = \begin{pmatrix} s_{11} & 0 & \cdots & \cdots & 0 \\ 0 & s_{22} & \ddots & & \vdots \\ \vdots & \ddots & \ddots & \ddots & \vdots \\ \vdots & & \ddots & \ddots & 0 \\ \vdots & & & \ddots & s_{N+1N+1} \\ 0 & \cdots & \cdots & \cdots & 0 \\ \vdots & & & & \vdots \\ 0 & \cdots & \cdots & \cdots & 0 \end{pmatrix} \Rightarrow S_q = \begin{pmatrix} 0 & \cdots & \cdots & \cdots & \cdots & 0 \\ \vdots & \ddots & \ddots & & & \vdots \\ \vdots & \ddots & s_{55} & \ddots & & \vdots \\ \vdots & & \ddots & 0 & \ddots & 0 \\ \vdots & & & \ddots & \ddots & 0 \\ 0 & \cdots & \cdots & \cdots & \cdots & 0 \\ \vdots & & & & & \vdots \\ 0 & \cdots & \cdots & \cdots & \cdots & 0 \end{pmatrix}$$

$$D_q = U S_q V^T$$

Reconstructed matrix D_q keeping only 5th singular value

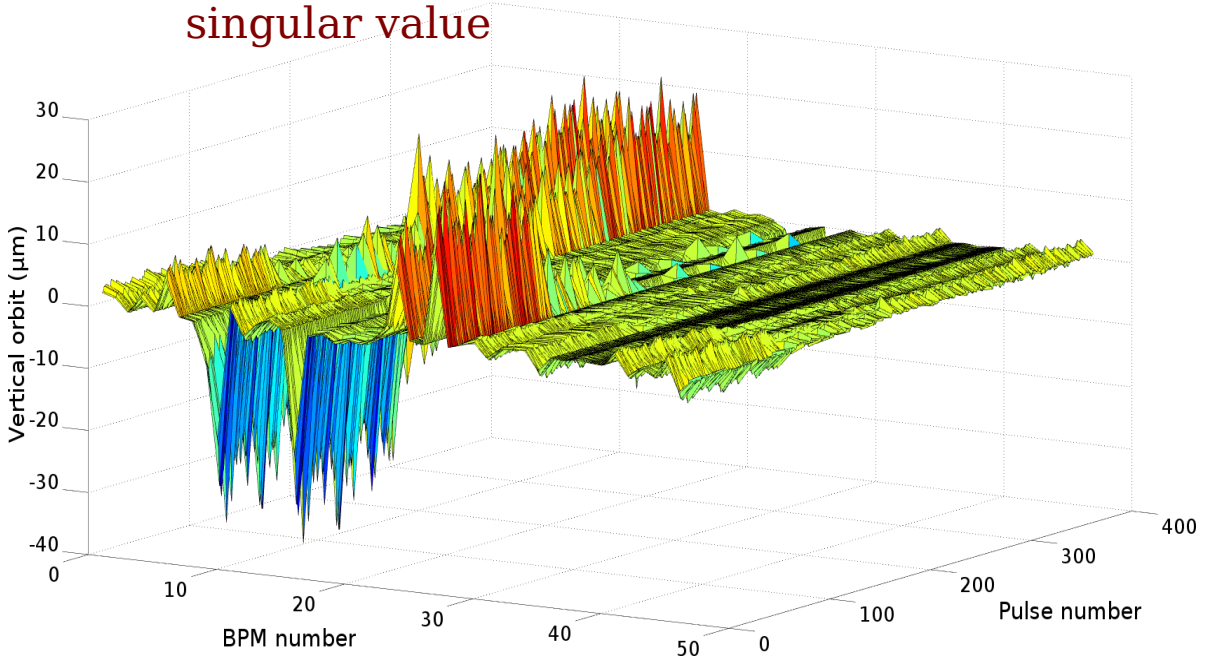

Future Plans

Corrections & SVD analysis

Corrections:

Update and Run One-to-One, DFS, WFS and wakefield knobs corrections.

SVD studies:

- There is much to learn about the system from an SVD analysis. SVD can:
  - Detect correlations (e.g., intensity-dependent orbit deflections, beam jitter, energy errors, ...)
  - Filter raw data and improve measurement precision (e.g., detect faulty BPMs, …)
  - Infer and identify the model of the system (e.g., reconstruct the response matrix, …)

Experimental Proposal:

- Refresh these studies for the new setup to characterise the updated system after the improvements in beam stability, charge stability, reduction of wakefield sources.
- Extend the studies to Damping Ring and Extraction Kicker.
- Apply Machine Learning Techniques and compare results with SVD analysis.

Flight Simulator

The lattice model and start-to-end simulations, should be developed in full integration with the Flight Simulator

- Update/Improve the existing one.
- Integrate and enable new functionalities and help automatization of key procedures
  - **Automatic response matrix measurement**
  - **Orbit Correction, DFS, WFS**
  - Tuning knobs, tuning bumps

CLEAR

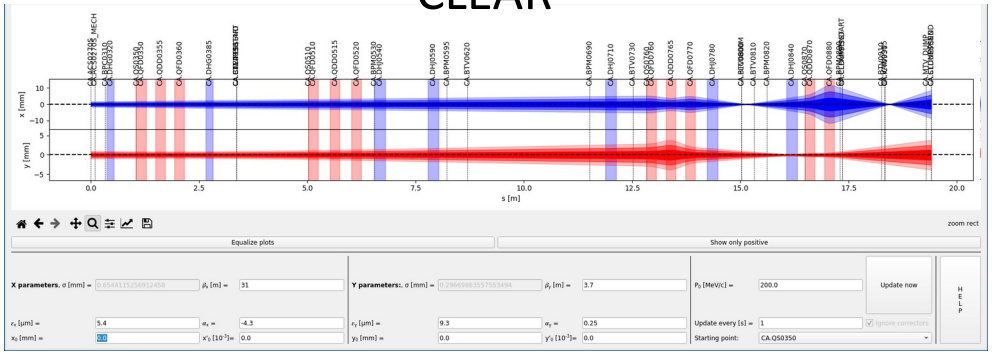

CLIC Beam-Based Alignment Tests at FACET

Dispersion-free Steering (DFS) proof of principle – March 2013

A. Latina, J. Pfingstner, E. Adli, D. Schulte

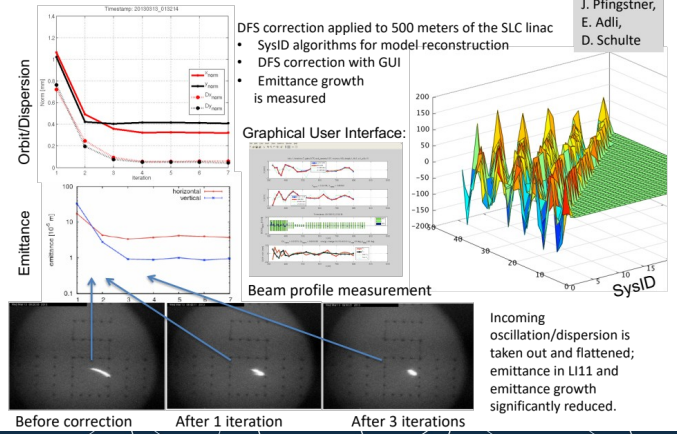

Thank you